Low Temperature Plasma
Technology Laboratory

**Antenna Mechanisms and
Electrostatic Fields in
Helicon Discharges**

Francis F. Chen

LTP-1212 December 2012

Electrical Engineering Department
Los Angeles, California 90095-1594

UNIVERSITY OF CALIFORNIA • LOS ANGELES

Antenna mechanisms and electrostatic fields in helicon discharges

Francis F. Chen, Electricial Engineering Department, University of California, Los Angeles, California, 90095-1594

ABSTRACT

The most efficient antennas for exciting helicon waves can be traced back to the so-called Nagoya Type III antenna. Its physical mechanism that couples radiofrequency (rf) energy to the plasma was explained by John Dawson in the 1970s but has not been published in readily accessible journals. Helical and Boswell-type antennas are modifications of this antenna. In all cases it is the current elements parallel to the dc magnetic field (B-field, $\mathbf{B_0}$) that are important: they create electrostatic fields (E-fields). Though whistler waves are purely electromagnetic, their confinement in a cylinder to form helicon waves causes them to be partly electrostatic. Computations of the E-fields in helicons are given to shown their importance.

I. Helicon antennas

In experiments on rf plugging of mirror machines, Watari *et al*.[1] found that one type of antenna excited much larger rf fields in the plasma than the others. The reason for this was not known until the antenna was used in the Dawson Separation Process for purifying uranium using ion cyclotron waves. John Dawson's explanation has been published only in a book celebrating his 60th birthday[2] and is repeated here. Figure 1 shows a full-wavelength Nagoya Type III antenna. Normally only half of this is used and is sufficient.

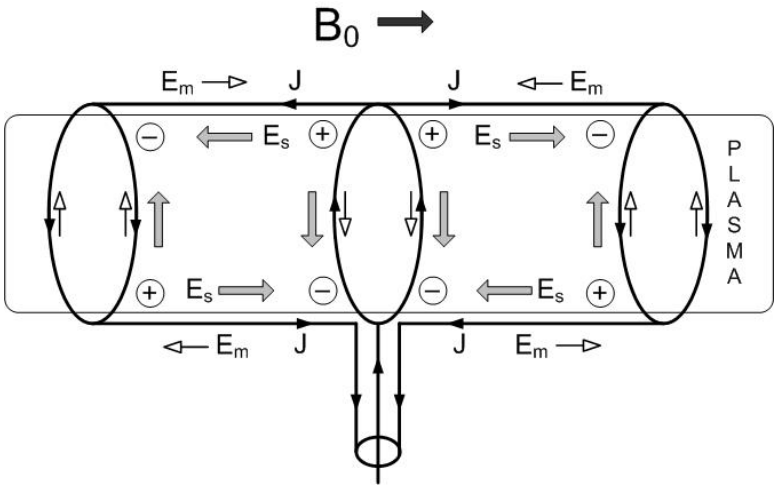

Fig. 1. Diagram of a Nagoya Type III antenna.

In a rising half-cycle, the rf current enters from the cable, splits in half at the center ring, and goes around the plasma to reach the top parallel leg. There it splits again and goes left and right to the two end rings, where the current again goes around the plasma to reach ground via the bottom parallel leg. Consider the top leg. As the current **J** rises, it generates a field $\mathbf{E_m}$ which opposes the rise. That field pushes electrons away from the center ring. Electrons then pile up near the end rings, leaving a positive space charge near the center ring. These charges generate an electrostatic field $\mathbf{E_s}$ pointing away from center. The field $\mathbf{E_s}$ builds up until it stops

the electron flow along $\mathbf{B_0}$. At the same time, the opposite currents and charges are created near the bottom leg. The antenna thus creates a pattern of space charges marked ⊕ and ⊖ on the diagram. These space charges in turn create a transverse E-field perpendicular to $\mathbf{B_0}$, as indicated by the heavy arrows. This vertical E-field is in the same direction as the $\mathbf{E_m}$ field of the ring currents but is much stronger, since the space charges were collected over the length of the antenna. The longer the antenna, the larger the space charge must be to cancel the field $\mathbf{E_m}$. Hence, the antenna amplifies the applied rf field by creating electrostatic fields. It can be shown[3] with a rectilinear model of the antenna that the amplification factor is approximately $(k_\perp^2/k_\parallel^2)$, where the k's are the antenna wavenumbers perpendicular and parallel to $\mathbf{B_0}$.

The Boswell antenna, shown in Fig. 2, is a modified Nagoya antenna with the top and bottom legs split into two wires so that the antenna consists of two separate halves. The advantage of this is that the antenna can be slipped around a cylindrical discharge tube without sliding it to the ends, which are blocked by vacuum lines.

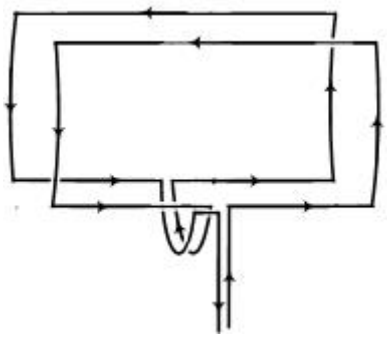

Fig. 2. Schematic of a Boswell antenna.

As shown by Miljak[4], helical antennas are Nagoya antennas twisted into right- or left-handed helices to better match the fields of the helicon wave. A "right-helical" antenna, with azimuthal mode number $m = +1$, is shown in Fig. 3. This antenna creates much higher plasma densities than the left-helical $m = -1$ antenna. The reason is not entirely clear, although the field patterns of the two are somewhat different[5]. The Nagoya antenna, being symmetric, generates both $m = +1$ and $m = -1$ fields, but the discharge is almost entirely due to the $m = +1$ mode.

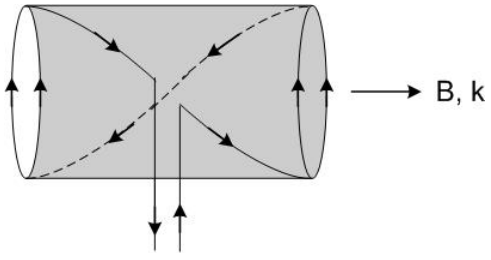

Fig. 3. Schematic of a right-helical antenna with wires which turn clockwise as one moves along **B**. If **k** is in the direction shown, this generates an $m = -1$ wave, which turns counterclockwise as seen by a stationary observer looking along **B**. If **k** is reversed, an $m = +1$ helicon would be excited.

In the $m = \pm 1$ case, the same field pattern simply rotates as seen by a stationary observer (Fig. 4a). The presence of electrostatic space charges can be seen from the convergence and divergence of the field lines at an intermediate radius. The azimuthally symmetric $m = 0$ helicon mode has an entirely different nature, as seen in Fig. 4b. The E-field lines change from solenoidal (electromagnetic) to radial (electrostatic) in every half cycle, with a mixture in between. Thus, the rf E-field there and the rf B-field are of equal importance. Figure 5 shows

examples of m = 0 antennas. The separated-loop antenna was used in a commercial helicon source[6], and the simple loop antenna of various numbers of turns is used in permanent-magnet helicon sources[7].

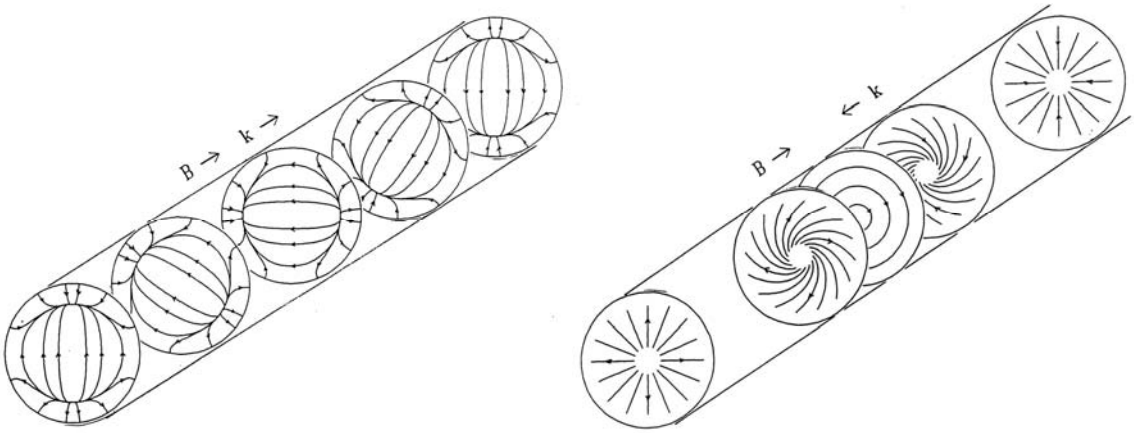

(a) (b)

Fig. 4. E-field patterns generated by an (a) m = 1 and (b) m = 0 antenna.

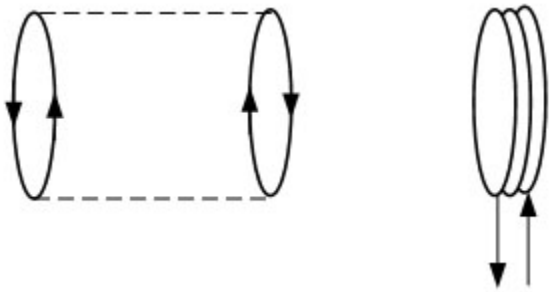

(a) (b)

Fig. 5. Examples of m = 0 antennas. (a) Separated loops with currents in the same or opposite directions; (b) a 3-turn loop antenna.

II. Electric fields

The strength of the E-fields in helicon discharges can be computed with the HELIC code of D. Arnush[8]. This user-friendly program computes in four seconds all the real and imaginary parts of **E**, **B**, and plasma current **J** of coupled helicon and Trivelpiece-Gould (TG) waves, and their magnitudes, in cylinders of specified radius and length, as long as $\mathbf{B_0}$ and plasma density n are uniform axially. The density, electron temperature T_e, and neutral pressure p can vary radially, and the type of antenna can be specified. The results are normalized to 1A of antenna current. (A normal current at 400W is about 20A.) Since the m = 1 and m = 0 modes are so different, we give examples of each. The TG mode is a problem, since it is electrostatic and will dominate the results, thus obscuring the electrostatic fields intrinsic to Nagoya Type III antennas which we wish to show. Fortunately, the HELIC code can separate the helicon and TG components for *infinite* cylinders, and the helicon E-fields can be seen separately in that case.

We first show these separated results for a uniform plasma: $n(r)$ = constant. Figure 6 shows the B and E magnitudes for the helicon (H) wave alone, and Fig. 7 shows these for the TG mode alone. The H wave is dominated by its r and ϕ components, while the TG mode is almost

entirely radial. Evident in Fig. 7 is the very strong E-field of the TG mode that is responsible for the efficient rf absorption of helicon sources. These curves were computed for a 5.16 cm diam tube, 2 m long, bounded by conducting endplates, with a 12 cm long half-helical antenna at the midplane. The radial profiles were taken inside the antenna. Assumed parameters were B_0 = 0.1T, $n = 10^{12}$ cm^{-3}, KT_e = 3 eV, rf frequency = 13.56 MHz, and p = 15 mTorr of argon.

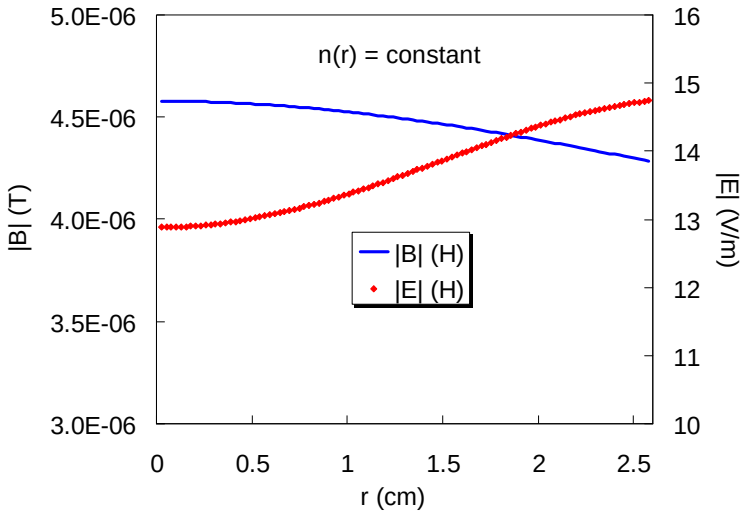

Fig. 6. RF magnetic field (line) and electric field (points, right scale) for the helicon wave alone in a uniform plasma. Note that the scales have suppressed zeroes. All calculations are for 1A of antenna current.

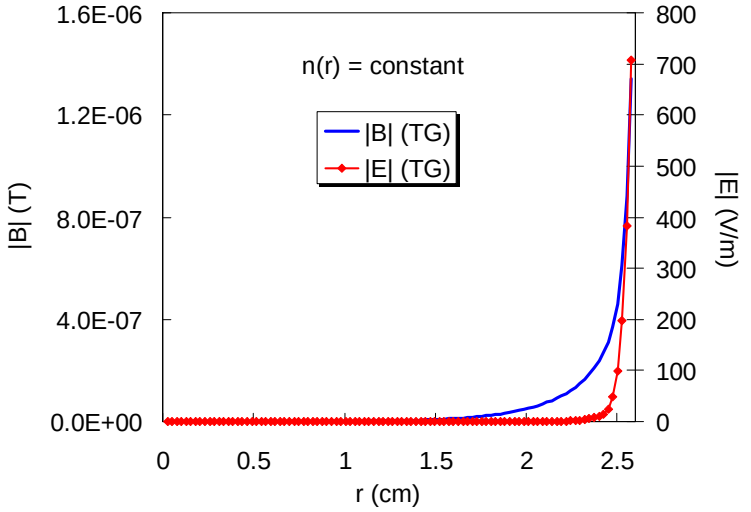

Fig. 7. RF magnetic field (line) and electric field (points, right scale) for the TG wave alone in a uniform plasma.

Since the m = 1 and m = 0 modes have different E-field patterns, as shown in Fig. 4, we next compare the wave fields for these azimuthal modes. For the m = 0 mode, we compute the fields for the actual experimental device used in Ref. 7. The tube is 2.58 cm in radius and 2.54 cm long, open at the bottom for injection of the plasma into a large chamber. The rf **B** and **E** fields are shown in Fig. 8 calculated with the "universal" $n(r)$ profile found by Curreli and Chen[9]. The dominant component of **E** is E_r, which drives the azimuthal current J_ϕ. It is seen in Fig. 9 that J_ϕ follows E_r at small radii but is diminished by ion current at large radii.

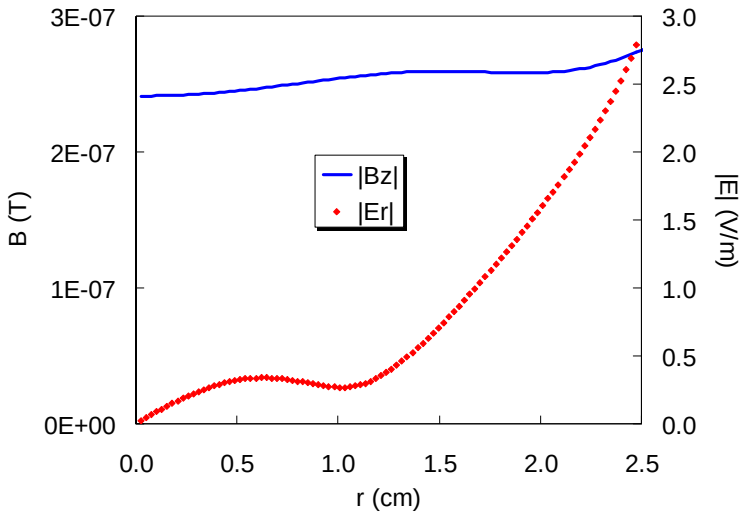

Fig. 8. Dominant components of **B** (line) and **E** (points) generated by an $m = 0$ antenna. Parameters are 13.56 MHz, 15 mTorr Ar, KT_e = 2.4 eV, n(peak) = 10^{11} cm^{-3}, and B_0= 60G (.006T).

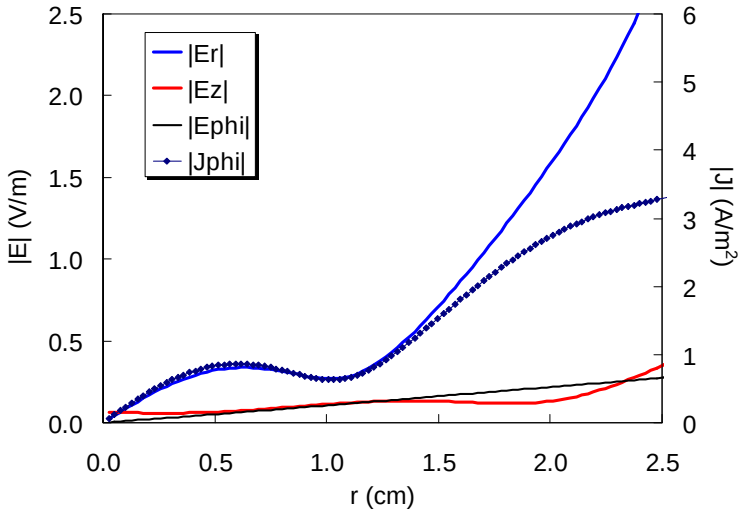

Fig. 9. Components of the **E** of Fig. 8 compared with J_ϕ (points, right scale).

For the $m = 1$ case, we computed examples for a half-helical antenna 12 cm long in the same conditions as in Fig. 6, but with $n(r)$ given by the "universal" profile of Ref. 9. The dominant **B** and **E** components are shown in Fig. 10. At the high field of 0.1T, the TG mode dominates, creating the very large E-field at the edge.

In spite of the large values of E in the TG mode, the energy density of the rf E-field is much smaller than that of the rf B-field. This is shown in Fig. 11.

III. SUMMARY

Dawson's mechanism for the Nagoya Type III antenna and its variations shows how electrostatic fields are generated in discharges with $m = \pm 1$ antennas. The mechanism that creates E-fields with $m = 0$ antennas is different and not yet explained on the same level. The magnitude of the E-field of the TG mode in a small helicon discharge can reach 8 V/cm with only 1A of antenna current, but the rf energy density is still dominated by the rf B-field.

This paper is a tribute to two old friends, Don Arnush and John Dawson.

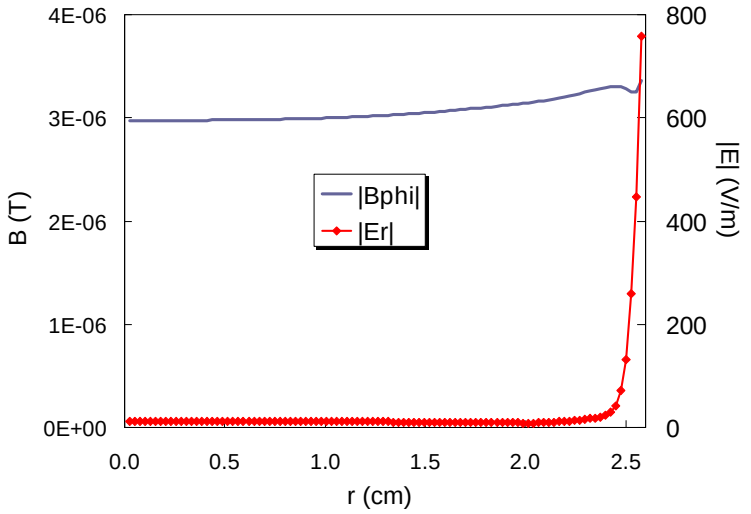

Fig. 10. Dominant components of **B** (line) and **E** (points, right scale) for an m = 1 antenna under the same conditions as in Fig. 6.

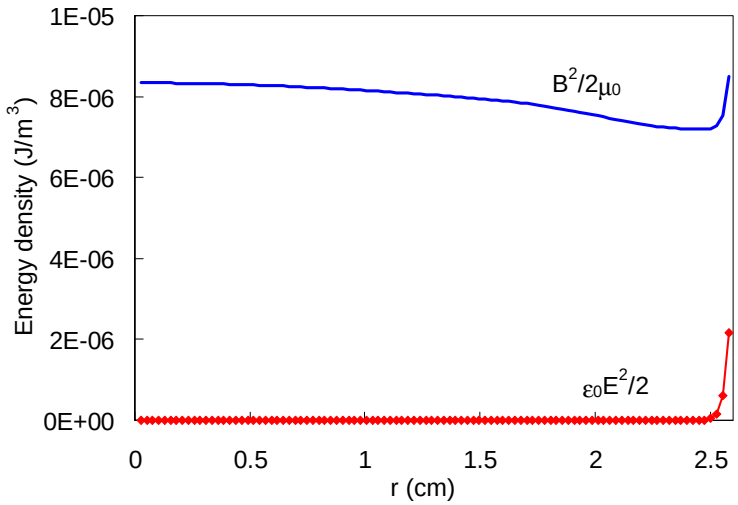

Fig. 11. Energy densities of the rf B- and E-fields (not including $\mathbf{B}_0$), plotted on the same scale, for the same uniform plasma as in Fig. 6.

REFERENCES

[1] T. Watari, T. Hatori, R. Kumazawa, S. Hidekuma, T. Aoki, T. Kawamoto, M. Inutake, S. Hiroe, A. Nishizawa, K. Adati, T. Sato, T. Watanabe, H. Obayashi,, and K. Takayama, Phys. Fluids 21, 2076 (1978).

[2] F.F. Chen, *Double Helix: The Dawson Separation Process*, in "From Fusion to Light Surfing", ed. by T. Katsouleas (Addison-Wesley, New York, 1991), Chap. 14.

[3] F.F. Chen, *Radiofrequency field enhancement near ion gyroresonance*, TRW Report Task II-3552 (1981), available at http://www.ee.ucla.edu/~ffchen/Archive/Chen095.pdf.

[4] D.G. Miljak and F.F. Chen, Plasma Sources Sci. Technol. **7**, 61 (1998).

[5] F.F. Chen, *Helicon Plasma Sources*, in "High Density Plasma Sources", ed. by Oleg A. Popov (Noyes Publications, Park Ridge, NJ, 1995), Chap. 1.

[6] G.R. Tynan, A.D. Bailey III, G.A. Campbell, R. Charatan, A. de Chambrier, G. Gibson, D.J. Hemker, K. Jones, A. Kuthi, C. Lee, T. Shoji, and M. Wilcoxson, J. Vac. Sci. Technol. A **15**, 2885 (1997).

[7] F.F. Chen, Phys. Plasmas **19**, 093509 (2012).

[8] D. Arnush, Phys. Plasmas **7**, 3042 (2000). The HELIC program is available at http://www.ee.ucla.edu/~ltptl/presentations.htm

[9] D. Curreli and F.F. Chen, Phys. Plasmas **18**, 113501 (2011).